EUROPEAN ORGANIZATION FOR NUCLEAR RESEARCH

March 29, 2013

Minimal physical constraints on the angular distributions of two-body boson decays

Pietro Faccioli[1,2)], Carlos Lourenço[3)], João Seixas[1,2)] and Hermine K. Wöhri[3)]

Abstract

The angular distribution of the two-body decay of a boson of unknown properties is strongly constrained by angular momentum conservation and rotation invariance, as well as by the nature of the detected decay particles and of the colliding ones. Knowing the border between the "physical" and "unphysical" parameter domains defined by these "minimal constraints" (excluding specific hypotheses on what is still subject of measurement) is a useful ingredient in the experimental determinations of angular distributions and can provide model-independent criteria for spin characterizations. In particular, analysing the angular decay distribution with the general parametrization for the $J = 2$ case can provide a model-independent discrimination between the $J = 0$ and $J = 2$ hypotheses for a particle produced by two real gluons and decaying into two real photons.

[1)] Laboratório de Instrumentação e Física Experimental de Partículas (LIP), Lisbon, Portugal
[2)] Physics Department, Instituto Superior Técnico (IST), Lisbon, Portugal
[3)] European Organization for Nuclear Research (CERN), Geneva 23, Switzerland

1 Introduction

Measurements of the angular distributions of particle decays give unique insights into the underlying fundamental interactions and play a central role in the determination of coupling properties, in the verification of production models and even in the discovery and identification of new particles.

However, some of the most basic properties of the decay distributions are ignored in many experimental analyses of Standard-Model (SM) couplings of vector bosons, Drell–Yan and quarkonium production. Only recently some general characteristics of the angular distribution have been systematically addressed, highlighting the importance of the choice of polarization axis [1, 2, 3], revealing the existence of general frame-independent relations [4, 5] and precisely defining the shape of the allowed parameter domain [6].

In this paper we determine the physically-allowed parameter domains of the two-body decays of bosons, generalizing a previous study limited to the parity-conserving dilepton decays of $J = 1$ particles [6]. Considering a broad range of physical processes involving two-body decays, we derive model-independent constraints that the parameters of the decay distributions must obey. These "minimal physical constraints" (MPCs) are determined only by angular momentum conservation, by rotation invariance and by the identities of the initial- and final-state particles, minimizing hypotheses on the nature and properties of the decaying particle.

A very interesting by-product of this study is the observation that $J = 0$ and $J = 2$ bosons produced by two real gluons and decaying into two real photons have well-separated physically-allowed parameter spaces. Therefore, these two spin options can be discriminated with a model-independent procedure, describing the measured angular decay distribution using the general parametrization for the $J = 2$ case and studying the extracted anisotropy parameters (only two in the case of the polar projection) as contours in the parameter space.

The paper is organized as follows. After discussing the formalism used for the description of the two-body decay angular distribution (Sec. 2) and, in particular, its polar projection (Sec. 3), we address in detail the case of a $J = 1$ particle (Sec. 4), considering the most general two-body decay as well as, specifically, the decay into a fermion-antifermion pair, including possible parity-violating effects. In Sec. 5 we discuss the $J = 2$ case, focusing on the polar projection of the decay distribution and giving examples of how the MPCs affect the angular parameters for different production and decay modes. Finally, in Sec. 6 we illustrate the utility of the MPCs in analyses aimed at characterizing the spin of new particles, such as the heavy diphoton resonance recently discovered at CERN [7, 8].

2 The two-body decay distribution of a boson

Using the notations defined in Fig. 1, the decay of a particle T of total angular momentum quantum number J into two observed particles X_1 and X_2 of angular

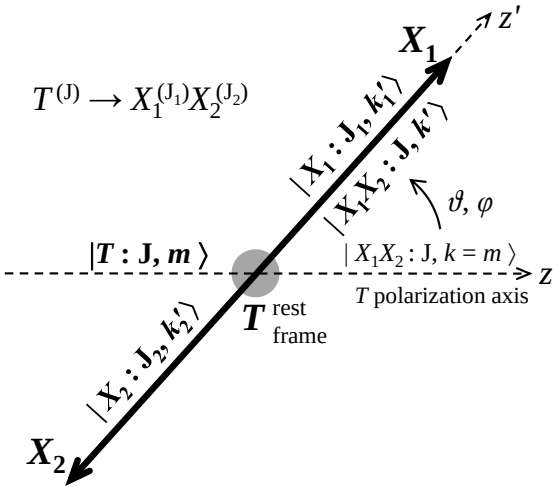

Figure 1: Sketch of the $T \to X_1 X_2$ decay, specifying notations for axes, angles and angular momentum states.

momenta J_1 and J_2 has the following angular distribution:

$$W(\cos\vartheta, \varphi) = \sum_{\substack{|k'| \leq \min(J, J_1+J_2) \\ |m| \leq J,\ |n| \leq J}} \rho^{k'}_{m,n}\ \mathcal{D}^{J}_{m,k'}(\cos\vartheta, \varphi) \mathcal{D}^{J*}_{n,k'}(\cos\vartheta, \varphi)\,, \tag{1}$$

with

$$\rho^{k'}_{m,n} = \sum_{\substack{|k_1'| \leq J_1,\ |k_2'| \leq J_2 \\ k_1' + k_2' = k'}} \left\langle \mathcal{A}^{*}_{m,k_1',k_2'} \mathcal{A}_{n,k_1',k_2'} \right\rangle\,. \tag{2}$$

In these equations, k_1' and k_2' are the angular momentum projections of X_1 and X_2 along their common direction in the T rest frame (z' axis), and m is the T angular momentum projection along the chosen T quantization axis z (for example the T momentum in the laboratory, or the direction of one or the other colliding beam, or the average of the two). The angular functions $\mathcal{D}^{J}_{m,k'}$ are the elements of the Wigner matrix, which applies the axis rotation $xyz \to x'y'z'$ to the X_1X_2 angular momentum state, re-expressing the pure $J_{z'}$ eigenstate $|X_1X_2 : J, k'\rangle$ into a combination of J_z eigenstates $|X_1X_2 : J, k\rangle$. The rotation angles are the (polar and azimuthal) decay angles ϑ and φ, defined as the angles formed by X_1 (or by X_2) with respect to the axis z and a suitably defined xz plane (for example the "production plane", containing the momenta of the colliding beams and of the decaying particle).

The amplitudes $\mathcal{A}_{m,k_1',k_2'}$, depending on the elementary couplings in the production and decay process considered, determine the allowed combinations of initial- and final-state "helicities" (here we define the helicity of a particle as its total angular momentum projection along a specified axis). For example, in the decays of SM vector gauge bosons into fermions, all amplitudes with opposite fermion spin projections, $\mathcal{A}_{m,\pm 1/2,\mp 1/2}$, vanish in the limit of massless fermions because of helicity conservation. In Eq. 2, the amplitude products $\mathcal{A}^{*}_{m,k_1',k_2'} \mathcal{A}_{n,k_1',k_2'}$ appear in a weighted average over

all subprocesses contributing to the production of T, with weights proportional to their relative yields. The complex coefficients $\rho^{k'}_{m,n}$ form, for each k', a hermitian matrix ($\rho^{k'}_{m,n} = \rho^{k'*}_{n,m}$) with trace unity, often referred to as "spin density matrix".

It is worth reminding that the relation $|J_1 - J_2| \leq J \leq J_1 + J_2$ is not necessarily satisfied when the decay products X_1 and X_2 have a relative orbital angular momentum (for example, a $J = 2$ particle can decay into two fermions with $J_1 = J_2 = 1/2$ and relative orbital angular momentum $L \geq 1$). However, L does not play an explicit role in the expression of the decay distribution, Eq. 1, because its projection along the quantization axis of the decay products (z') is always zero.

3 The polar projection of the decay distribution

The polar projection of the general decay angular distribution, Eq. 1, is obtained by integrating over φ. Given the general identity

$$\int \mathrm{Re}\left[\mathcal{C}\ \mathcal{D}^{J*}_{m,k'}(\cos\vartheta,\varphi)\mathcal{D}^{J}_{n,k'}(\cos\vartheta,\varphi)\right] d\varphi = 0\ , \tag{3}$$

for $n \neq m$, where $\mathcal{C}$ is any combination of complex amplitudes not depending on φ, the integrated expression is

$$w(\cos\vartheta)\ =\ \sum_{\substack{|k'|\leq \min(J,J_1+J_2)\\ |m|\leq J}} \sigma_{m,k'}\left[d^{J}_{m,k'}(\cos\vartheta)\right]^2\ , \tag{4}$$

where $d^J_{m,k'}$ are the reduced Wigner matrix elements, functions of $\cos\vartheta$, and $\sigma_{m,k'} \equiv \rho^{k'}_{m,m}$. This expression only depends on the squared moduli of the helicity amplitudes ("diagonal" $\rho^{k'}_{m,m}$ terms). Therefore, any information about the interference between different angular momentum eigenstates composing the initial state is lost in the polar projection of the distribution.

The decaying particle can be a coherent or an incoherent superposition of eigenstates (as exemplified in Sec. 4 of Ref. [3]). These two physically different cases lead to different azimuthal anisotropies, properly reflected in Eq. 1, but not to different polar anisotropies, thereby being indistinguishable in the polar projection. While the maximum number of observable parameters of the full distribution is 8 for $J = 1$ (5 if the particle is observed inclusively, without referring the polarization axes to possible accompanying particles in the event) and 24 for $J = 2$ (14 for inclusive observation), the corresponding polar projections have only 2 and 4 measurable parameters, respectively. The azimuthal dependence of the distribution obviously vanishes when the particle is produced in $2 \to 1$ processes and the polarization axis z is chosen along the direction of the colliding particles.

For a generic J, the polar angle projection can be expressed in terms of $2J$ independent observable coefficients, λ_i, as

$$w(\cos\vartheta \mid \vec{\lambda})\ =\ \frac{1}{2}\,\frac{1+\sum_{i=1}^{2J}\lambda_i\,(\cos\vartheta)^i}{1+\sum_{j=1}^{J}\frac{\lambda_{2j}}{2j+1}}\,. \tag{5}$$

4 The $J = 1$ specific case

The most general form of the two-body decay angular distribution of a $J = 1$ particle is

$$\begin{aligned} W(\cos\vartheta,\varphi) \;=\; & \frac{3/(4\pi)}{(3+\lambda_\vartheta)}\,(1+\lambda_\vartheta\cos^2\vartheta\,+ \\ & +\lambda_\varphi\sin^2\vartheta\cos2\varphi+\lambda_{\vartheta\varphi}\sin2\vartheta\cos\varphi \\ & +\lambda_\varphi^\perp\sin^2\vartheta\sin2\varphi+\lambda_{\vartheta\varphi}^\perp\sin2\vartheta\sin\varphi \\ & +2A_\vartheta\cos\vartheta+2A_\varphi\sin\vartheta\cos\varphi+2A_\varphi^\perp\sin\vartheta\sin\varphi)\,, \end{aligned} \tag{6}$$

where

$$\begin{aligned} \lambda_\vartheta =& 1/D\,[4\rho^0_{0,0}+\rho^{+1}_{+1,+1}+\rho^{-1}_{+1,+1}+\rho^{+1}_{-1,-1}+\rho^{-1}_{-1,-1} \\ & -2(\rho^{+1}_{0,0}+\rho^{-1}_{0,0}+\rho^{0}_{+1,+1}+\rho^{0}_{-1,-1})]\,, \\ \lambda_\varphi =& 2/D\,\mathrm{Re}(\rho^{+1}_{+1,-1}+\rho^{-1}_{+1,-1}-2\rho^{0}_{+1,-1})\,, \\ \lambda_\varphi^\perp =& 2/D\,\mathrm{Im}(\rho^{+1}_{+1,-1}+\rho^{-1}_{+1,-1}-2\rho^{0}_{+1,-1})\,, \\ \lambda_{\vartheta\varphi} =& \sqrt{2}/D\,\mathrm{Re}[\rho^{+1}_{+1,0}+\rho^{-1}_{+1,0}-2\rho^{0}_{+1,0} \\ & -(\rho^{+1}_{0,-1}+\rho^{-1}_{0,-1}-2\rho^{0}_{0,-1})]\,, \\ \lambda_{\vartheta\varphi}^\perp =& \sqrt{2}/D\,\mathrm{Im}[\rho^{+1}_{+1,0}+\rho^{-1}_{+1,0}-2\rho^{0}_{+1,0} \\ & -(\rho^{+1}_{0,-1}+\rho^{-1}_{0,-1}-2\rho^{0}_{0,-1})]\,, \\ A_\vartheta =& 1/D\,(\rho^{+1}_{+1,+1}-\rho^{-1}_{+1,+1}+\rho^{-1}_{-1,-1}-\rho^{+1}_{-1,-1})\,, \\ A_\varphi =& \sqrt{2}/D\,\mathrm{Re}(\rho^{+1}_{+1,0}-\rho^{-1}_{+1,0}+\rho^{+1}_{0,-1}-\rho^{-1}_{0,-1})\,, \\ A_\varphi^\perp =& \sqrt{2}/D\,\mathrm{Im}(\rho^{+1}_{+1,0}-\rho^{-1}_{+1,0}+\rho^{+1}_{0,-1}-\rho^{-1}_{0,-1})\,, \\ & \text{with}\;\; D=\;\rho^{+1}_{+1,+1}+\rho^{-1}_{+1,+1}+\rho^{+1}_{-1,-1}+\rho^{-1}_{-1,-1} \\ & \qquad +2(\rho^{+1}_{0,0}+\rho^{-1}_{0,0}+\rho^{0}_{+1,+1}+\rho^{0}_{-1,-1})\,. \end{aligned} \tag{7}$$

The parameters $\lambda_\varphi^\perp$, $\lambda_{\vartheta\varphi}^\perp$ and $A_\varphi^\perp$ are of physical interest only if the particle is observed in an exclusive production channel, taking into account the momenta of accompanying particles in a specific event topology, in which case at least one other physical plane, besides the one formed by the colliding beams, can be chosen as a meaningful reference for the definition of the azimuthal angle.

The physically observable parameter domain is defined by the following MPCs, obtained using Eqs. 2 and 7:

$$\begin{aligned} \lambda^{\otimes2}_{\vartheta\varphi}+2(\tilde{A}^2+A^2_\vartheta) &\le 2(1+\lambda_\vartheta)\,, \\ \lambda^{\otimes2}_{\vartheta\varphi} &\le 2(1+\lambda_\vartheta)\left[1-\sqrt{2A^{\otimes2}_\varphi}\right], \\ \lambda^{\otimes2}_{\vartheta\varphi} &\le 2(1+\lambda_\vartheta)(1-|A_\vartheta|)\,, \\ 4A^2_\vartheta &\le (1+\lambda_\vartheta)^2\,, \\ \tilde{A}^2+A^{\otimes2}_\varphi &\le 1\,, \end{aligned}$$

$$
\begin{aligned}
\tilde{A}^2 + A_\varphi^{\otimes 2} + \lambda_\vartheta^2 &\leq 1 \;\text{ if }\; \lambda_\vartheta < 0\,, \\
A_\varphi^{\otimes 2} &\leq (1+\lambda_\vartheta)\left(1 - \sqrt{A_\vartheta^2 + \lambda_\varphi^{\otimes 2}}\right), \\
\tilde{A}^2 + \lambda_\varphi^{\otimes 2} &\leq 1\,, \\
\lambda_{\vartheta\varphi}^2 + \tilde{A}^2 &\leq (1+\lambda_\varphi)(1+\lambda_\vartheta)\,, \\
4A_\varphi^2 &\leq (1+\lambda_\varphi)^2\,, \\
2A_\varphi^2 + \lambda_\varphi^{\perp 2} &\leq 1\,, \\
2A_\varphi^2 + (1-2\lambda_\varphi)^2 &\leq 1 \;\text{ if }\; \lambda_\varphi > 1/3\,, \\
2A_\varphi^2 + (1-2\lambda_\varphi)^2 + \lambda_\varphi^{\perp 2} &\leq 1 \;\text{ if }\; \lambda_\varphi > 1/2\,, \\
2A_\varphi^2 + \lambda_\varphi^{\otimes 2} &\leq 1 \;\text{ if }\; \lambda_\varphi < 0\,,
\end{aligned}
\tag{8}
$$

where

$$
X_i^{\otimes} \equiv \sqrt{X_i^2 + X_i^{\perp 2}} \quad \text{and} \quad \tilde{A} \equiv \sqrt{A_\vartheta^2 + A_\varphi^2 + A_\varphi^{\perp 2}}\,.
$$

The last 6 inequalities also apply after the simultaneous substitutions $A_\varphi \to A_\varphi^\perp$, $\lambda_{\vartheta\varphi} \to \lambda_{\vartheta\varphi}^\perp$ and $\lambda_\varphi \to -\lambda_\varphi$.

In the case of the decay into a fermion-antifermion pair via an intermediate vector boson (when $k' = 0$, i.e. $\rho_{m,n}^0 = 0$, is forbidden because of helicity conservation, valid in the limit of massless fermions or heavy initial state), the MPCs can be written as

$$
\begin{aligned}
G(\lambda_\varphi, \lambda_\vartheta) &\geq 2(\lambda_{\vartheta\varphi}^{\perp 2} + A_\varphi^2)\,, \\
G(-\lambda_\varphi, \lambda_\vartheta) &\geq 2(\lambda_{\vartheta\varphi}^2 + A_\varphi^{\perp 2})\,, \\
G\left(\sqrt{\lambda_\varphi^{\otimes 2} + A_\vartheta^2}, \lambda_\vartheta\right) &\geq 2(\lambda_{\vartheta\varphi}^{\otimes 2} + A_\varphi^{\otimes 2})\,, \\
G\left(-\sqrt{\lambda_\varphi^{\otimes 2} + A_\vartheta^2}, \lambda_\vartheta\right) &\geq 0\,,
\end{aligned}
\tag{9}
$$

with $G(X,Y) = 1/2\,[(1+X)^2 - (Y+X)^2]$.

As a result of the inequalities themselves, the left-side terms (G functions) are bound between 0 and 1, and the right sides of the inequalities are sums of quantities all individually included between 0 and 1. These inequalities become equivalent to those presented in Ref. [6] when only the three parity-conserving observables λ_ϑ, λ_φ and $\lambda_{\vartheta\varphi}$ are considered. We note that a misprint occurred in Eq. 3 of Ref. [5], where the factors $\sqrt{2}/(2\mathcal{D})$ starting the expressions of A_φ and $A_\varphi^\perp$ should be replaced by $\sqrt{2}/\mathcal{D}$. This misprint does not affect any of the subsequent formulas (frame transformation, frame-invariant asymmetries) involving A_φ and $A_\varphi^\perp$. With this correction, the expressions of Ref. [5], valid in the special case of di-fermion decays with fermion helicity conservation, where $\rho_{m,n}^0 = 0$, are a particular version of the expressions presented in Eq. 7.

Figure 2 shows the two-dimensional projections of the physical parameter domain for inclusive observations (λ_ϑ, λ_φ, $\lambda_{\vartheta\varphi}$, A_ϑ and A_φ), in the most general case and in the specific case of fermion-antifermion decays.

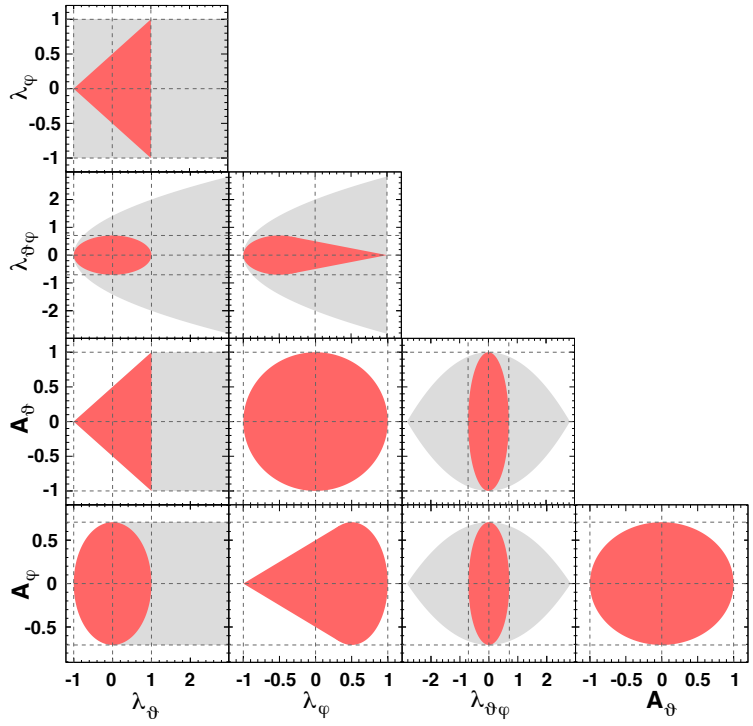

Figure 2: Allowed parameter regions of the two-body decay distribution of an inclusively observed $J = 1$ boson. The largest areas (gray) represent the most general domain while the inner areas (red) represent the di-fermion decay case. In the most general case there are no upper bounds on λ_ϑ and $|\lambda_{\vartheta\varphi}|$. The $\lambda_\vartheta < 3$ bound was added for improved visibility.

5 The polar projection of the $J = 2$ case

The polar projection of the two-body decay distribution of a $J = 2$ particle is described by four independent parameters (defined by Eq. 5),

$$\begin{aligned}
\lambda_1 &= 4(\alpha^-_{22} - 2\alpha^-_{11} + 4\alpha^-_{12})/D\,, \\
\lambda_2 &= 6(\alpha^+_{22} - \alpha^+_{00} - 2\alpha^+_{02} - 2\alpha^+_{11} + 4\alpha^+_{01})/D\,, \qquad (10)\\
\lambda_3 &= 4(\alpha^-_{22} + 4\alpha^-_{11} - 4\alpha^-_{12})/D\,, \\
\lambda_4 &= (\alpha^+_{22} + 9\alpha^+_{00} + 6\alpha^+_{02} + 16\alpha^+_{11} - 24\alpha^+_{01} - 8\alpha^+_{12})/D\,,
\end{aligned}$$

$$\text{with}\quad D = \alpha^+_{22} + \alpha^+_{00} + 6\alpha^+_{02} + 4\alpha^+_{11} + 8\alpha^+_{12}\,, \qquad (11)$$

$$\begin{aligned}
\text{and}\quad \alpha^\pm_{i,j} \;&=\; \sigma_{i,j} + \sigma_{j,i} + \sigma_{-i,-j} + \sigma_{-j,-i} \\
&\pm (\sigma_{i,-j} + \sigma_{-j,i} + \sigma_{-i,j} + \sigma_{j,-i})\,. \qquad (12)
\end{aligned}$$

The physical domain of the $\lambda_1, \ldots, \lambda_4$ parameters depends on the type of decay products and on the production mechanism. Figure 3 shows the physically allowed regions of the $J = 2$ parameter space corresponding to MPCs of increasing strength. The largest areas, in gray, represent the most general case: only angular momentum conservation and rotation invariance are imposed. The more restricted areas, in colour, represent the effects of selecting one of two specific physics hypotheses: either the decay products are real photons ($\sigma_{m,\pm1} = 0$ for any m), or the decaying boson

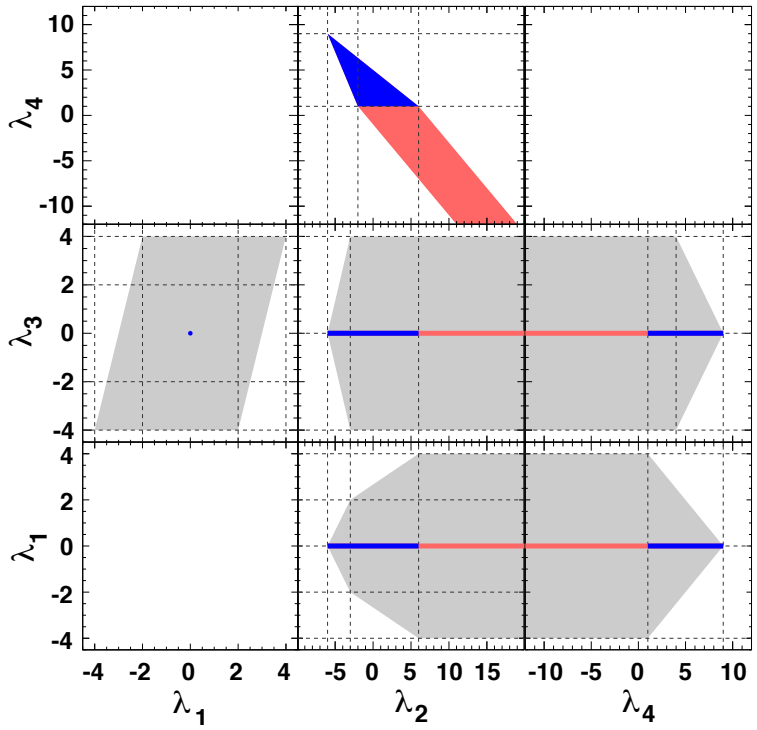

Figure 3: Allowed parameter regions of the polar projection of the two-body decay distribution of a $J = 2$ boson. The largest areas (gray) represent the most general domain. The intermediate areas (red+blue) represent any of two equivalent cases: T decays into two real photons; T is produced alone from the scattering of two real gluons. The smallest areas (blue) represent the case where both hypotheses are satisfied. There is no upper bound on λ_2 and no lower bound on λ_4.

is produced alone from the scattering of two real (transversely polarized) gluons ($\sigma_{\pm 1,m} = 0$ for any m when the polarization axis is chosen along the scattering direction of the gluons). The smallest areas, in blue, show the particularly interesting case when *both* of these hypotheses apply: the boson is produced in gluon-gluon fusion and decays into two photons.

Figure 4 shows two other interesting physical cases. The intermediate areas, in colour, represent the case in which the boson decays into two $J = 1/2$ fermions, while the smallest areas, in blue, also impose the extra condition that the boson is produced alone from the scattering of two real gluons. When either the elementary production process is initiated by two identical particles or the decay products are two identical particles, the parity-violating terms λ_1 and λ_3 obviously vanish, resulting in simple lines or dots as allowed regions in the two-dimensional projected domains.

6 Spin characterization of a heavy di-photon resonance

Hypotheses on the properties of the fundamental couplings involved can, obviously, further restrict the allowed regions or even fix the values of the λ_i parameters for

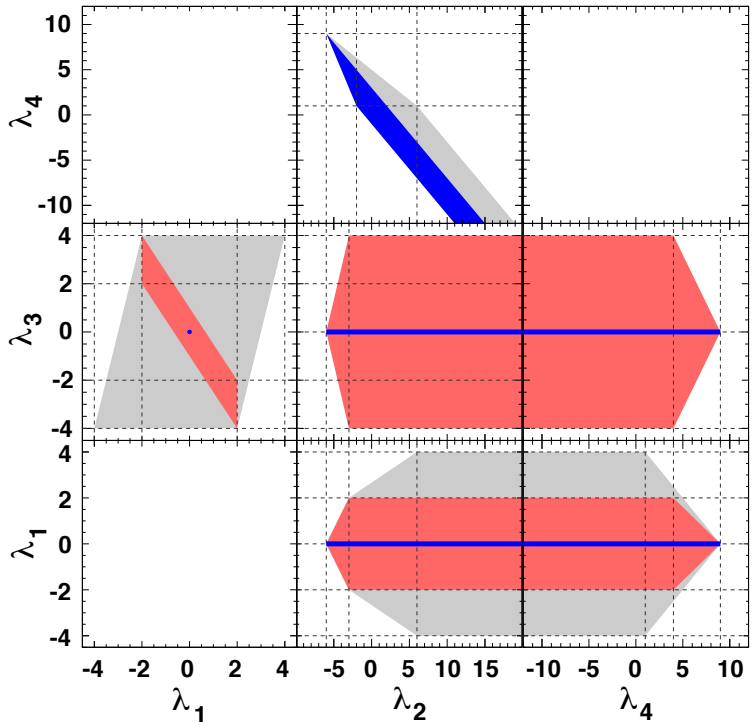

Figure 4: Allowed parameter regions of the polar projection of the two-body decay distribution of a $J = 2$ boson. The largest areas (gray) represent the most general domain. The intermediate areas (red+blue) represent the case in which T decays into two $J = 1/2$ fermions. The smallest areas (blue) correspond to the hypothesis that T is produced alone from the scattering of two real gluons *and* decays into two fermions. There is no upper bound on λ_2 and no lower bound on λ_4.

the $J = 2$ particle. For example, considering the gluon-gluon to photon-photon case (where $\lambda_1 = \lambda_3 = 0$), the hypothesis of a graviton-like $J = 2$ particle interacting with SM bosons with no helicity flip [9] (corresponding to the conditions $\sigma_{0,m} = \sigma_{m,0} = 0$ for any m) leads to $\lambda_2 = 6$ and $\lambda_4 = 1$, the rightmost vertex of the blue triangle in the λ_2–λ_4 plane, top panel of Fig. 3. This particular model has been considered as a possible interpretation of the "Higgs-like particle" recently discovered by the ATLAS and CMS experiments [7, 8]. We will now analyze this physical example as an illustration of the usefulness of the MPCs.

To determine the angular momentum quantum number of the new resonance, it is interesting to note that a particle produced (alone) from the scattering of two real gluons and decaying into two real photons always decays with a significant polar anisotropy ($\vec{\lambda} \neq 0$) with respect to the scattering direction of the gluons, as long as $J \neq 0$. This completely model-independent result, shown in Fig. 3 for the $J = 2$ case (λ_4 is always ≥ 1), can be generalized to other J values. Since the $J = 1$ case is excluded by the Landau–Yang theorem, let us consider $J = 3$ and $J = 4$.

The polar projection of the di-photon decay distribution of a $J = 3$ particle

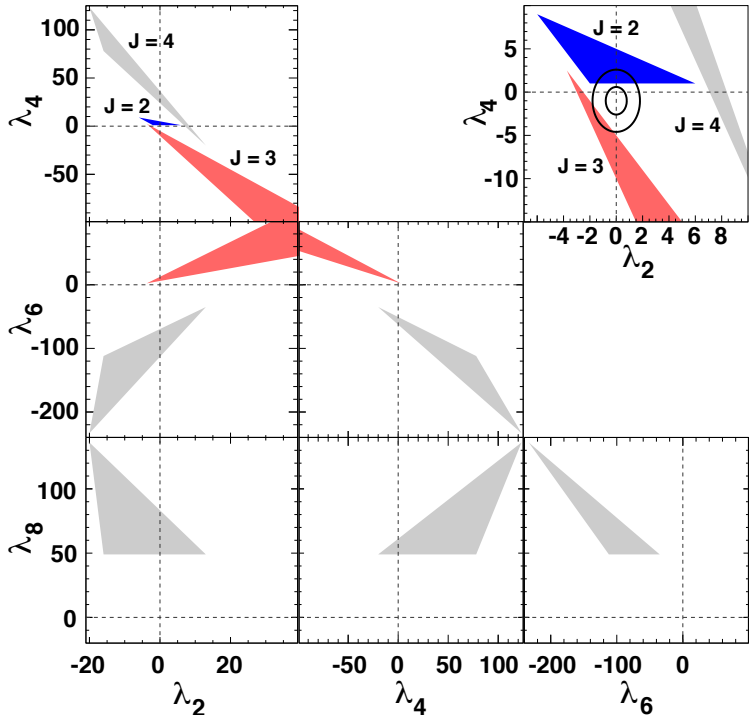

Figure 5: Allowed regions for the parameters of the polar projection of the decay distribution of a particle produced by gluon-gluon fusion and decaying into two photons. The three different shades indicate, from darkest (blue) to lightest (gray), the $J = 2$, 3 and 4 cases. In the $J = 3$ case there are no upper bounds on λ_2 and λ_6 and no lower bound on λ_4. The top-right panel shows a zoom of the top-left panel.

produced by gluon-gluon fusion is described by the parameters

$$\begin{aligned} \lambda_2 &= 3(3\alpha^+_{00} + 10\alpha^+_{02} - 5\alpha^+_{22})/D\,, \\ \lambda_4 &= 10(-3\alpha^+_{00} - 6\alpha^+_{02} + \alpha^+_{22})/D\,, \\ \lambda_6 &= (25\alpha^+_{00} + 30\alpha^+_{02} + 9\alpha^+_{22})/D\,, \\ \text{with}\ \ D &= 4\alpha^+_{22}\,. \end{aligned} \tag{13}$$

The corresponding $J = 4$ decay parameters are

$$\begin{aligned} \lambda_2 &= 4(-45\alpha^+_{00} - 160\alpha^+_{02} + 52\alpha^+_{22})/D\,, \\ \lambda_4 &= 10(111\alpha^+_{00} + 312\alpha^+_{02} - 32\alpha^+_{22})/D\,, \\ \lambda_6 &= -140(15\alpha^+_{00} + 32\alpha^+_{02} + 4\alpha^+_{22})/D\,, \\ \lambda_8 &= 49(25\alpha^+_{00} + 40\alpha^+_{02} + 16\alpha^+_{22})/D\,, \\ \text{with}\ \ D &= 9\alpha^+_{00} + 40\alpha^+_{02} + 16\alpha^+_{22}\,. \end{aligned} \tag{14}$$

In both cases the parity-violating λ_i parameters (odd i) vanish. The parameter domains for $J = 2$, 3 and 4 are shown in Fig. 5. The minimum distance from the origin ($\vec{\lambda} = 0$, corresponding to $J = 0$) increases from $J = 2$ to $J = 3$ to $J = 4$ and, in general, should increase with J, reflecting the stronger polarization imposed by the limitation of the initial- and final-state helicities to $|m| \leq 2$ and $|k'| \leq 2$.

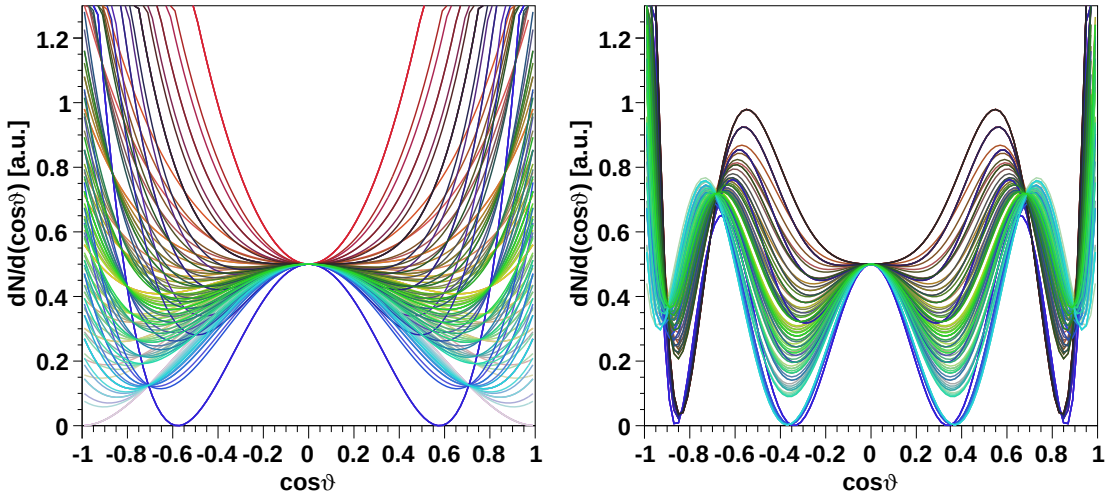

Figure 6: Physically allowed $\cos\vartheta$ distributions for $J = 2$ (left) and $J = 4$ (right) bosons produced by gluon-gluon fusion and decaying into two photons. For clarity of representation, all distributions are normalized to the same value at $\cos\vartheta = 0$.

It is interesting to note that the three domains have no intersections between them and also not with the $J = 0$ point ($\vec{\lambda} = 0$). Therefore, a sufficiently-precise measurement of the di-photon decay distribution can provide an unambiguous spin characterization, independent of specific hypotheses on the identity of the particle.

The experimental precision needed to achieve a significant discrimination obviously depends on J and on the actual values of the polarization parameters, defined by the identity of the particle. The top-right panel of Fig. 5 includes two ellipses that illustrate two putative measurements, the radii representing their uncertainties. The outer one excludes the $\lambda_2 = 6$, $\lambda_4 = 1$ point, eliminating the hypothesis that the decaying boson is a graviton-like $J = 2$ particle of the kind discussed in Ref. [9]. However, it does not rule out other hypothetical $J = 2$ (or even $J = 3$) bosons, corresponding to parameters (calculable from the relevant couplings) closer to the $\lambda_2 = \lambda_4 = 0$ origin (that represents the isotropic distribution of a $J = 0$ particle). The inner ellipsis illustrates another hypothetical measurement, sufficiently precise to exclude the full $J = 2$ and $J = 3$ domains, thereby leading to the model-independent spin characterization of a $J = 0$ particle.

Figure 6 illustrates the dependence of the observable $\cos\vartheta$ distribution on J, taking as examples the $J = 2$ and 4 cases. The curves were obtained by scanning the (respectively, two- and four-dimensional) physical domains of the λ_i parameters. The recognizable difference in shape between any single $J = 2$ curve and any single $J = 4$ curve shows that it is always possible, with a sufficiently-precise measurement, to unambiguously determine one and only one spin value.

As shown in Fig. 5, the physically-allowed parameter regions of the $J = 0, 2, 3$ and 4 cases do not intersect each other, a non-trivial observation that can potentially lead to significant improvements in some of the LHC data analyses. However, it should be kept in mind that these parameter regions have been established under the (commonly-assumed) condition that the boson under study is produced in a $2 \to 1$ (leading order) process. While one can often argue (in the context of differential

cross sections, for instance) that next-to-leading order contributions can be neglected in first approximation, this might not be defendable in studies aimed at measuring the spin of a new resonance. Indeed, from a polarization perspective, the $2 \to 1$ and $2 \to 2$ cases are completely different. Even if the extra emitted particles have almost zero momentum, the simple symmetry of the $2 \to 1$ reaction is broken and the polarization, which is a topological property, changes in a drastic way. In the $J = 2$ case, for instance, there would no longer be any restriction of the most general parameter domain, as can be seen in Fig. 3 (top panel), where the most general λ_2 vs. λ_4 region (gray) coincides with the "intermediate region" (red plus blue). The most constrained parameter space (blue), which, in particular, excludes the unpolarized option, is only obtained when we complement the two-photon decay restriction with the $2 \to 1$ production hypothesis.

7 Concluding remarks

A complete knowledge of how the parameters of a decay angular distribution are constrained and mutually correlated simply by rotation invariance, angular momentum conservation and the identities of the initial- and final-state particles (i.e., with minimal or no hypotheses on the nature, properties and/or polarization of the decaying particle itself) can bring important benefits to experimental analyses. In polarization measurements, significant violations of such MPCs (in this case defined as constraints not imposing any condition on the polarization itself) can indicate the existence of systematic biases in the analysis, related, for example, to the acceptance determination or to the modelling and subtraction of the backgrounds.

Moreover, the analysts can (and should) embed the prior knowledge of the physical bounds into the measurement, according to the Bayesian reasoning. This procedure can appreciably change the significance of the result when the observation is interestingly at the border of the parameter space. This is usually the case, for example, of the SM vector gauge bosons, strongly polarized (either transversely or longitudinally) both when produced directly in parton-parton scattering (Drell–Yan-like processes) and when coming from the decay of massive particles (top quark, heavy Higgs boson).

Finally, the physical parameter domain for a given process depends on the spin of the decaying particle. Its detailed knowledge can, therefore, provide a model-independent instrument for the spin characterization of newly discovered particles. This approach may require larger acquired event samples with respect to binary comparisons between specific physical hypotheses, but provides a more model-independent and unequivocal answer to the basic physical question.

P.F. and J.S. acknowledge support from Fundação para a Ciência e a Tecnologia, Portugal, under contracts SFRH/BPD/42343/2007 and CERN/FP/109343/2009.

References

[1] P. Faccioli, C. Lourenço, J. Seixas and H.K. Wöhri, Phys. Rev. Lett. 102, 151802 (2009).

[2] P. Faccioli, C. Lourenço and J. Seixas, Phys. Rev. D 81, 111502(R) (2010).

[3] P. Faccioli, C. Lourenço, J. Seixas and H.K. Wöhri, Eur. Phys. J. C 69, 657 (2010);

[4] P. Faccioli, C. Lourenço and J. Seixas, Phys. Rev. Lett. 105, 061601 (2010).

[5] P. Faccioli, C. Lourenço, J. Seixas and H.K. Wöhri, Phys. Rev. D 82, 096002 (2010).

[6] P. Faccioli, C. Lourenço, J. Seixas and H.K. Wöhri, Phys. Rev. D 83, 056008 (2011).

[7] ATLAS Collaboration, Phys. Lett. B 716, 1 (2012).

[8] CMS Collaboration, Phys. Lett. B 716, 30 (2012).

[9] Y. Gao et al., Phys. Rev. D 81, 075022 (2010).